Aquaculture 616 (2026) 743684

Contents lists available at ScienceDirect

Aquaculture

journal homepage: www.elsevier.com/locate/aquaculture

The phylogenetics and pathogen population dynamics of infectious hypodermal and hematopoietic necrosis virus (IHHNV) in global shrimp populations

Emmanuel Ofori-Amponsah [a,*], Maria Andrade Martinez [b,c], Michael T. Meehan [a,1], Kelly Condon [b,c]

[a] College of Medicine and Dentistry, James Cook University, Townsville, Australia
[b] College of Science and Engineering, James Cook University, Townsville, Australia
[c] JCU AquaPATH, James Cook University, Townsville, Australia

ARTICLE INFO

Keywords:
IHHNV
Phylogenetics
Shrimp
Capsid
NS1

ABSTRACT

Infectious Hypodermal and Hematopoietic Necrosis Virus (IHHNV) has posed a persistent threat to global shrimp aquaculture since its emergence in the 1980s, with transmission exacerbated by intensified farming and international trade. While previous studies have focused on regional outbreaks, the global evolutionary dynamics of IHHNV remain poorly understood. Here, we analyse 126 IHHNV capsid protein sequences (107 sequences extracted from GenBank and 19 newly collected sequences from northern Queensland, Australia) and 63 NS1 gene sequences (44 from GenBank and 19 from northern Queensland, Australia) collected from 12 countries between 1986 and 2022. Bayesian coalescent analyses estimate a mean nucleotide substitution rate of 4.5×10^{-4} (95% HPD 2.8×10^{-4}, 6.4×10^{-4}) substitutions/site/year for the capsid region and 1.9×10^{-4} (95% HPD 1.1×10^{-4}, 2.8×10^{-4}) for NS1, consistent with earlier region-specific results. The time to the most recent common ancestor was dated to the early 1980s (95% HPD: 1976–1986). Demographic reconstruction revealed periods of exponential growth in the 1990s and early 2000s, followed by a decline in the mid-2010s. Phylogenetic analysis revealed marked genetic diversity and strong geographic structuring, with some evidence of international viral exchange. Distinct regional SNP patterns mirrored the phylogenetic structure, supporting geographically constrained viral evolution and diversification. The high evolutionary rates and structured global distribution of IHHNV underscore the need for continued molecular surveillance and enhanced biosecurity to mitigate the risk of future outbreaks.

1. Introduction

Infectious Hypodermal and Hematopoietic Necrosis Virus (IHHNV) is a single-stranded DNA virus within the *Penstylhamaparvovirus* genus of the *Parvoviridae* family (Shike et al., 2000; Yu et al., 2021). IHHNV emerged during the 1980s whereby it caused substantial mortality in *Penaeus stylirostris*, and was reported in association with runt deformity syndrome (RDS) with reduced growth and body deformities in *Penaeus vannamei* (Bell and Lightner, 1984; Castille et al., 1993) and *Penaeus monodon* broodstock (Primavera and Quinitio, 2000).

The IHHNV genome is approximately 4 kb long and encodes three open readings frames (ORFs): NS1 (2001 bp); NS2 (1092 bp); and the capsid protein (990 bp) (Rai et al., 2012; Shike et al., 2000). Of the three distinct genotypes, genotypes I and II are infectious, while genotype III is non-infectious and represents endogenous viral elements (EVEs) (Aranguren Caro et al., 2022; Dhar et al., 2022).

Accurate and rapid detection of IHHNV is critical for broodstock screening and disease surveillance in shrimp aquaculture. In addition to conventional PCR and qPCR assays, several isothermal amplification methods have been developed. Loop-mediated isothermal amplification (LAMP) approaches include the in-situ DIG-labelled LAMP (ISDL) assay, which detects IHHNV directly in tissue sections with higher sensitivity and faster turnaround than traditional in situ hybridization (Jitrakorn et al. 2016); a double-target colorimetric LAMP (D-LAMP) that amplifies two genomic regions of *Penaeus stylirostris* densovirus while reducing false positives from EVEs (Arunrut et al. 2019); and a real-time triplex

* Corresponding author.
[1] Joint senior author.

https://doi.org/10.1016/j.aquaculture.2026.743684
Received 2 November 2025; Received in revised form 19 December 2025; Accepted 19 January 2026
Available online 21 January 2026

LAMP monitored by a turbidimeter, suitable for routine field screening with performance comparable to qPCR (Arunrut et al. 2024). Recombinase polymerase amplification (RPA) assays have also been developed, including a real-time RPA targeting nucleotides 868–1000 (Xia et al., 2015) and a lateral flow dipstick (LFD) assay targeting nucleotides 3094–3214 (Jaroenram and Owens, 2014) of GenBank no. 272315 respectively. Collectively, these methods demonstrate the diagnostic and epidemiological significance of IHHNV detection and provide tools for effective monitoring and management of infection in shrimp populations.

Following IHHNV's first detection in juvenile blue shrimp (*P. stylirosis*) in Hawaii during the early 1980s (Lightner et al., 1983), the virus was subsequently detected in *P. stylirostris* in Mexico in 1990 (Lightner, 1992a, 1992b), and other Central and South American countries in the late 1980s and early 1990s (dos Santos Braz et al., 2009; Lightner, 1992b; Lightner et al., 1983). The early disease outbreaks caused by IHHNV highlighted the virus's pathogenicity and prompted a major shift in culture practices, replacing the larger but highly susceptible *P. stylirostris* with the more resilient *P. vannamei*, despite the latter's comparatively slower growth (Alday-Sanz et al., 2020; Dhar et al., 2019; Fulks, 1992). The change in culture species to *P. vannamei* reduced the impact of IHHNV on global shrimp production (Wyban, 2007). In the early 1990s, IHHNV was confirmed in black tiger shrimp (*P. monodon*) in Australia (Krabsetsve et al., 2004; Owens, 1992) and was later reported throughout Southeast Asia and the Pacific, with detections in the Philippines by 1996 (Belak et al., 1998) and in Thailand by 2000 (Chayaburakul et al., 2004; Tang et al., 2003). An eastward distribution of IHHNV continued through the 2000s, with reports from Indonesia (2000) (Sunarto et al., 2004), China (2001) (Yang et al., 2007), India (2009) (Praveen Rai et al., 2009) and Korea (2011) (Kim et al., 2011). In Africa, non-infectious forms of IHHNV (EVEs) have been reported in *P. monodon* from Madagascar (2000) (Tang et al., 2003) and Mozambique (2000) (Tang and Lightner, 2006), as well as Tanzania (2006) (Tang and Lightner, 2006). The recent detection of IHHNV in *L. vannamei* from Canada (2019) and the United Kingdom (2019) (Canada, 2019; CEFAS, 2019) underscore continued international spread, which has likely been historically facilitated by global trade, transboundary brood stock movement, and the intensification of shrimp farming practices (Lightner, 1996; Lightner, 1999).

The status of IHHNV as a pathogen of concern is varied, with inconsistent documented impacts on growth, health, and survival in wild and farmed shrimp (Arbon et al., 2022; Jaroenram and Owens, 2014; Saksmerprome et al., 2010). Despite the long history of IHHNV detection, understanding of the virus's global population structure and evolutionary dynamics is limited. Previous phylogenetic studies have explored the genetic diversity and evolutionary rate of IHHNV in specific regions, estimating substitution rates ranging from $\sim 1.39 \times 10^{-4}$ (Robles-Sikisaka et al., 2010) to 1.55×10^{-3} (Jaroenram et al., 2015) substitutions/site/year. Robles-Sikisaka et al. (2010) found greater genetic diversity than previously reported, with effective population size changes closely aligned with epizootiological records Jaroenram et al. (2015), focusing on Australian isolates, inferred past population dynamics, noting that the effective number of infections gradually declined after 1991, followed by a recovery in 1996, and remained stable from 2003 onwards. However, studies such as Robles-Sikisaka et al. (2010) and Jaroenram et al. (2015) included endogenous viral elements (EVEs), which may confound evolutionary inferences. Moreover, most prior work has focused on either the capsid or NS1 gene, with limited global sampling, thereby constraining our understanding of the broader evolutionary dynamics, dispersal patterns, and demographic history of IHHNV.

This study analyses a globally diverse dataset of IHHNV sequences, including newly generated isolates from northern Queensland, Australia. We applied stringent filtering criteria to exclude EVEs as well as other problematic sequences. We analysed both capsid and NS1 genes to reconstruct evolutionary relationships, estimate substitution rates, and infer historical population dynamics. Our results provide new insight into the global structure, diversification, and demography of IHHNV, with implications for viral surveillance and control in aquaculture.

2. Materials and methods

2.1. Sequence data collection and processing

2.1.1. GenBank data retrieval

Capsid, NS1 and whole-genome sequences of Infectious Hypodermal and Hematopoietic Necrosis Virus (IHHNV) were retrieved from GenBank (Retrieved August 13, 2024, from https://www.ncbi.nlm.nih.gov/genbank). Inclusion criteria required sequences to be complete or > 80% of genome length, annotated with collection date and host species, and supported by published metadata. Only sequences derived from shrimp hosts were retained (Table 1). Sequences were excluded if they lacked collection dates or showed evidence of being endogenous viral elements (EVEs) which can distort phylogenetic relationships, artificially elongate branch lengths, and bias substitution-rate estimates (Holmes, 2011; Zhong et al., 2025). To minimise these effects, we first assembled a larger alignment that included all available IHHNV sequences, including those annotated or suspected as EVEs. This alignment was inspected in Geneious Prime 2024.0.3 (Dotmatics, V.2024.0.3) to identify sequences that showed EVE-like features, such as clustered SNPs, or SNP patterns that mirrored verified EVEs. ORFs from these suspected sequences were then BLASTed against a verified IHHNV EVE (DQ228358) sequence in GenBank, and sequences with high nucleotide identity across the ORF (>95%) were classified as EVEs and excluded from downstream analyses.

For whole genomes that met these criteria, the capsid and NS1 gene regions were extracted for separate analyses. Accession numbers, collection years, host species, and geographic origins of all sequences were recorded and summarised in Table 1 and Supplementary Tables 1 and 2 (Excluded and Included Sequences.pdf in ONLINE_RESOURCE_5_SUPPLEMENTARY, https://doi.org/10.5281/zenodo.17085148).

2.1.2. Australian sequences from this study

2.1.2.1. Sample collection and sequencing. An additional 19 IHHNV-positive samples were collected between 2018 and 2022 from shrimp on commercial farms in Queensland, Australia. DNA was extracted using the MagCORE Max (Applied Biosystems) kit on a KingFisher™ magnetic particle processor (Life Technologies) following the manufacturer's protocol. Samples with high copy number (Ct < 20) of IHHNV determined by qPCR analysis (Cowley et al., 2018) were submitted for Sanger sequencing. Amplicons for sequencing were prepared by using overlapping PCR primers (Silva et al., 2014). PCR products were analysed by gel electrophoresis on a 1.5% TAE agarose gel using Safe Imager 2.0 Blue-light Transilluminator (Life Technologies). Amplicons of expected size were cut from the gel and purified using the Bioline Isolate II PCR and gel kit (BIO-52060) following the manufacturer's instructions. Purified products were submitted for Sanger sequencing using the capillary separation process to the Australian Genome Research Facility (AGRF). Each amplicon was sequenced at least twice (forward and backward direction). Primer sequences are available in Table 2 of supplementary data.

2.1.2.2. Bioinformatics and genome assembly. ABI files of sequence reads were downloaded from the AGRF sample submission platform into the Geneious Prime Bioinformatics program. Chromatograms were observed for sequence quality and contigs of high quality (>90% confidence) denovo assembled. Assemblies were inspected manually to ensure agreement in sequence via overlapping primer position to ensure

Table 1
Summary of IHHNV sequences used in this study.

Country	Location	Years/Timespan	N		Species	Reference
			Capsid	NS1		
Australia	Queensland	2008	6	3	*P. monodon*	Moody et al. (Unpublished, NCBI)
Australia	North Queensland	2018–2022	19	19	*P. monodon*	JCU AquaPath Lab
Brazil	Rio Grande do Norte	2013	1	1	*P. vannamei*	(Silva et al., 2014)
China	Zhejiang Province	2014	5	5	*P. monodon, P. vannamei*	(Wei et al., 2015)
China	Sheyang	2011	2	2	*P. monodon, P. vannamei*	Fei et al. (Direct Submission, NCBI)
China	Shanghai	2012	2	2	*P. vannamei*	Chai and Wang (Direct Submission, NCBI)
China	Fujian	2008	1	1	*P. vannamei*	Wu et al. (Direct Submission, NCBI)
Ecuador	Not reported	2003	1	1	*P. vannamei*	(Hsia et al., 2003)
Ecuador	Santa Elena	2019	1	1	*P. vannamei*	(Bajaña et al., 2022)
Ecuador	Guayas	2021	1	1	*P. vannamei*	(Aranguren Caro et al., 2022)
Mexico	Gulf of California	1998	1	1	*P. stylirostris*	(Shike et al., 2000)
Mexico	Gulf of California	2004–2005	47	0	*P. stylirostris, P. vannamei*	(Robles-Sikisaka et al., 2010)
Peru	Tumbes	2019, 2022	13	13	*P. vannamei*	(Salcedo-Mejía et al., 2021)
Peru	Tumbes and Piura	2021	6	6	*P. vannamei*	(Aranguren Caro et al., 2022)
Philippines	Not reported	2007–2009	9	0	*P. vannamei, P. monodon*	(Tang et al., 2009)
South Korea	Taean Peninsula	2010	2	0	*P. vannamei*	(Kim et al., 2011)
South Korea	West Coast	2010	1	1	*P. vannamei*	(Kim et al., 2012)
Taiwan	Not reported	2001, 2003	2	2	*P. monodon*	(Hsia et al., 2003)
USA	Hawaii	1986	1	1	*P. vannamei*	(Mari et al., 1993)
USA	Florida, Texas	2019	2	2	*P. vannamei*	(Dhar et al., 2022)
Venezuela	Nueva Esparta and Zulia States	2008, 2014	2	0	*P. vannamei*	(Fajardo et al., 2015)
Vietnam	Mekong Delta	2012	1	1	*P. monodon*	Trung et al. (Direct Submission, NCBI)

amplicons were not individual EVE fragments.

2.1.2.3. Source of shrimp samples. The 19 IHHNV-positive samples were collected within the operational surveillance activities conducted at JCU AquaPATH. All samples were sourced from commercial farms or hatcheries of *Penaeus monodon* in Queensland, Australia. Life stage of samples ranged from wild collected broodstock, post larvae and pond-reared stock. Farms in this region operate under typical sub-tropical conditions, with water temperatures during the sampling period (2018–2022) generally ranging between 15 and 30 °C, salinity between 15 and 38 ppt.

Stocking densities and aeration practices were consistent with commercial operations which are varied across the sector. No targeted environmental monitoring accompanied the sampling; therefore, only general farm-level environmental context is provided. Previous research investigating possible association of farm practice with IHHNV prevalence and load yielded limited association.

2.2. Sequence alignment and SNP analysis

2.2.1 Multiple sequence alignment

44 whole-genome sequences, 63 capsid genes from GenBank and 19 Queensland isolates were aligned using the MUSCLE 5.1 algorithm in Geneious Prime 2024.0.3 (Dotmatics, V.2024.0.3). Capsid and NS1 regions were separately extracted from whole genome sequences and aligned to ensure consistent alignment of homologous regions. Final alignments were used to generate a maximum likelihood phylogenetic tree, which was exported in NEXUS format for TempEst analyses.

2.2.1. Single nucleotide polymorphisms (SNPs) detection

Single Nucleotide Polymorphisms (SNPs) were identified in our capsid alignment using the 'Find Variants' tool in Geneious Prime 2024.0.3 (Dotmatics, V.2024.0.3) with a minimum variant frequency threshold of 10%. The 10% threshold was chosen to prioritise high-frequency polymorphisms while reducing the likelihood of spurious variants arising from sequencing errors or misalignments. Each SNP was annotated as synonymous or non-synonymous following in silico translation of coding regions. Regional specificity of SNPs was assessed to identify lineage-defining variants or geographically structured polymorphisms.

2.2.2. Genetic similarity analysis

To assess genetic relatedness, a percent identity matrix was generated from the aligned capsid and NS1 sequences using Geneious Prime 2024.0.3 (Dotmatics, V.2024.0.3). The matrix provided pairwise comparisons of nucleotide sequences, calculating the percentage of identical bases between isolates and was used to evaluate intra- and inter-regional sequence similarity.

2.3. Phylogenetic and demographic inference

2.3.1. Substitution model selection

To determine the best-fitting nucleotide substitution model for phylogenetic analysis, the capsid and NS1 alignments in fasta formats were analysed using MEGA v.11 (Molecular Evolutionary Genetics Analysis) (FASTA-formatalignmentcapsidgenome in ONLINE_RESOURCE_1_GENOME ALIGNMENT, FASTA-formatalignmentns1 genome in ONLINE_RESOURCE_1_GENOME ALIGNMENT, https://doi.org/10.5281/zenodo.17085148). Model selection was based on the Bayesian Information Criterion (BIC) using the maximum likelihood method.

2.3.2. Bayesian evolutionary analysis

2.3.2.1. Assessing temporal signal. Before running the full Bayesian evolutionary analysis, we assessed the temporal signal in each dataset using root-to-tip regression in TempEst v1.5.3 (Rambaut et al., 2016), rooting the tree using the correlation method to maximise the association between sampling time and divergence. A maximum likelihood phylogenetic tree in NEXUS format, containing branch lengths and sampling dates, was used as input (phylogenetictreecapsid.nex and phylogenetictreens1.nex in ONLINE_RESOURCE_2_TEMPEST, https://doi.org/10.5281/zenodo.17085148). This analysis evaluates whether genetic divergence correlates with sampling dates, indicating the suitability of applying molecular clock models in phylogenetic inference.

2.3.2.2. Mutation rate and effective population size. The nucleotide substitution rate and the historical effective number of infections were estimated using the BEAST software package (version 2.7.6) (Bouckaert et al., 2019). Analyses were performed separately for the capsid and NS1 datasets using the best-fitting nucleotide substitution model identified

Table 2
SNP Variations and Geographic Patterns in the Capsid Genome of IHHNV Isolates.

SNP Position	Codon Change	Amino Acid Change	Regions Observed
22	**G**CA → **A**CA	A → T	Mexico
125	**AC**T → **AA**T	T → N	Peru, Ecuador, Florida, Texas, Mexico
153	CA**A** → CA**G**	Q → Q	Peru, Ecuador, Florida, Texas, Mexico
300	AA**G** → AA**A**	K → K	Australia, Taiwan, China, Philippines
313	**A**TG → **T**TG	M → L	Ecuador, China, Philippines, Florida, Peru
366	TC**G** → TC**A**	S → S	Ecuador, Venezuela, Brazil, China, Philippines, South Korea, Mexico, Texas, Peru
405	GG**C** → GG**T**	G → G	Mexico, USA, Peru, Ecuador
412	**T**TT → **A**TT	F → I	Mexico
456	TT**T** → TT**C**	F → F	Mexico
519*	AA**A** → AA**G**	K → K	China, Mexico
553*	**T**CA → **A**CA	S → T	South Korea
597	TT**C** → TT**T**	F → F	Texas, Peru, Ecuador
714	GG**T** → GG**C**	G → G	Australia
718	**T**TA → **A**TA	L → I	Mexico
721	**A**AA → **C**AA	K → Q	Mexico
823	**AA**T → **CA**T	N → H	Texas, Peru, Ecuador
907/908	**GT**C → **AC**C	V → T	Ecuador, Philippines, Mexico, South Korea, USA
965	AA**A** → AG**A**	K → R	Australia

NB: Positions are numbered relative to the capsid gene alignment (nucleotide 1 = start of the capsid ORF, corresponding to positions 3037–4026 of the IHHNV reference genome, GenBank accession no. AF218266).
Amino Acids Included: Alanine **(A)**, Threonine **(T)**, Glutamine **(Q)**, Lysine **(K)**, Methionine **(M)**, Serine **(S)**, Glycine **(G)**, Phenylalanine **(F)**, Valine **(V)**, Arginine **(R)**, Histidine **(H)**, Leucine **(L).**
NB: *These SNP sites do not fall within our 10% variant tool threshold but were still considered because they appeared to be region-specific.

by MEGA v11. For both regions, a relaxed lognormal molecular clock model was employed with an exponential prior on the substitution rate (mean = 1.4×10^{-4} subs/site/year, informed by (Robles-Sikisaka et al., 2010)). A coalescent Bayesian Skyline model with five population intervals (dimensions) was used as the tree prior to infer past changes in effective population size (coalescent_bayesian_skyline_HKY_capsid.xml in CAPSID, coalescent_bayesian_skyline_HKY_ns1.xml in NS1, ONLINE_RESOURCE_3_BEAST_FILES, https://doi.org/10.5281/zenodo.17085148).

Each MCMC chain was run for 7×10^7 iterations, sampling every 1000 iterations, with the first 10% of iterations discarded as burn-in. Two independent chains using different random number seeds were run to ensure convergence. Parameter estimates and convergence diagnostics were assessed using TRACER v1.1.2 (Bouckaert et al., 2019), with a minimum effective sample size (ESS) of 200 required for all parameters (tmrca_substitutionrates_capsid.log in CAPSID and tmrca_substitutionrates_ns1.log in NS1, ONLINE_RESOURCE_3_BEAST_FILES). The effective number of infections parameter was expressed in units of generations per year, which is appropriate for viruses such as IHHNV. Results from this analysis were visualised in TRACER v1.7.2 and processed in R using the ggtree and ggplot2 packages (BSP_R_capsid_ns1.R in ONLINE_RESOURCE_4_R SCRIPTS, https://doi.org/10.5281/zenodo.17085148).

2.3.2.3. Maximum clade credibility (MCC) tree. To summarise the posterior distribution of trees generated after MCMC analysis, the posterior tree file was analysed using TreeAnnotator v2.7.5 (part of the BEAST package) to generate a maximum clade credibility (mcc) tree. Posterior probabilities were used to assess nodal support. Final trees were visualised in FigTree v1.4.4 with nodes below a posterior support threshold of 0.80 collapsed into polytomies for clarity (collapsedcapsidtree.nexus, collapsedns1tree.nexus ONLINE_RESOURCE_3_BEAST_FILES). Additional annotation and formatting were performed in R v4.2 using the ape and ggtree packages (capsid_circulartree_final.R, ns1_circulartree_final.R in ONLINE_RESOURCE_4_R SCRIPTS, https://doi.org/10.5281/zenodo.17085148). A schematic overview of the workflow is shown in Fig. 1.

3. Results

3.1. Sequence overview and alignment

A total of 126 IHHNV nucleotide sequences were analysed in this study. These included 19 new whole-genome sequences from northern Queensland, Australia, and 107 publicly available sequences retrieved from GenBank, comprising 44 whole genomes and 63 capsid-specific sequences. For downstream analysis, 63 NS1 regions were also extracted from the whole genomes. A summary of these sequences, including their location, number, host species, sampling dates and references are provided in Table 1. Details of the sequences have been recorded in Supplementary Table 1.

After quality control and manual extraction of coding regions, multiple sequence alignments were generated for both the capsid and NS1 regions. The final alignment for the capsid region was 990 base pairs (bp) in length for most sequences; however, nine were between 940 and 948 bp, and one sequence was 873 bp. All NS1 sequences were 2001 bp in length. These alignments formed the basis for phylogenetic, demographic, and genetic diversity analyses.

3.2. SNP detection and genetic similarity

A total of 19 single nucleotide polymorphisms (SNPs) were identified across the capsid alignment, using a minimum variant frequency threshold of 10%. Of these, 8 were synonymous and 11 were non-synonymous, with amino acid changes determined through in silico translation (Table 2). Despite the filtering threshold, several SNPs – particularly those in South Korean and Chinese isolates – appeared in fewer than 13 sequences but remained consistently present within their respective regional groupings.

Distinct patterns of geographic structuring were evident in the SNP data. Isolates from Peru, Mexico, the United States and Ecuador shared several polymorphisms, while specific SNPs were unique to Mexican sequences. Australian sequences carried distinct SNPs, some of which were also present in isolates from China and Taiwan.

For the NS1 region, five SNPs were identified (Table 3), two of which were non-synonymous and three synonymous. Most of these SNPs were present in isolates from the Americas whereas one (SNP 1509) was almost exclusive to Australian isolates, occurring only once outside this region in a Peruvian isolate. Although fewer SNPs were detected in the NS1 region compared with the capsid region, their geographic associations further support the presence of regionally structured viral populations.

A percent identity matrix generated from the aligned capsid sequences revealed high levels of intra-regional similarity, particularly within Australian, Peruvian, and Mexican clades. Most sequences within each region shared greater than 98% nucleotide identity, consistent with

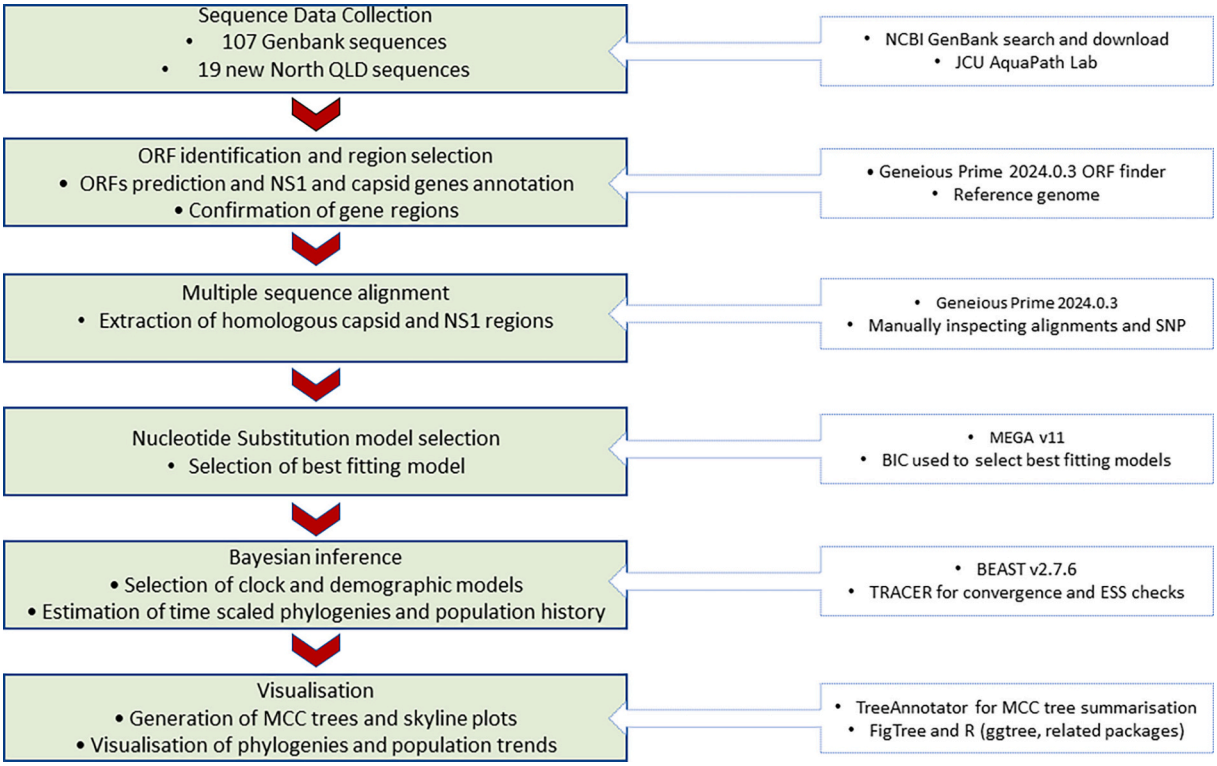

Fig. 1. Overview of the analytical workflow for phylogenetic and phylodynamic analysis of IHHNV sequences in this study. Summary of the processing pipeline, showing major steps and associated software used for ORF extraction, alignment, model selection, BEAST analysis, tree summarisation and visualisation.

Table 3
SNP Variations and Geographic Patterns in the NS1 Genome of IHHNV Isolates.

SNP Position	Codon Change	Amino Acid Change	Regions Observed
514	**C**AT → **G**AT	H → D	Peru, USA
742	**C**GA → **A**GA	R → R	Ecuador, Peru, South Korea, Texas
1072	**G**AC → **T**AC	D → Y	Ecuador, Peru, USA
1509	CT**C** → CT**A**	L → L	Australia, Peru (1 isolate)
1917	AA**G** → AA**A**	K → K	Ecuador, Peru

NB: Positions are numbered relative to the NS1 gene alignment (nucleotide 1 = start of the NS1 ORF, corresponding to positions 1095–3095 of the IHHNV reference genome, GenBank accession no. AF218266).
Amino Acids Included: Histidine **(H)**, Aspartic **(D),** Arginine **(R)**, Lysine **(K)**, Leucine **(L),** Tyrosine **(Y).**

the clustering patterns later observed in the phylogenetic tree. Notably, the 19 newly sequenced Australian isolates were genetically identical at the capsid SNP sites to the most recently reported Australian sequences in GenBank. These variants were unique to Australia.

3.3. Molecular evolutionary rates and divergence times

The best-fitting nucleotide substitution model for the capsid and NS1 alignments, as identified by MEGA v11 using the Bayesian Information Criterion (BIC), was the HKY model (Hasegawa et al., 1985) with gamma-distributed rate variation across four categories and a proportion of invariant sites (HKY + G + I). This model was subsequently applied in BEAST v2.7.6 to estimate evolutionary rates and divergence times.

Bayesian phylogenetic analysis of the capsid gene yielded a mean nucleotide substitution rate of 4.5×10^{-4} substitutions per site per year (95% HPD 2.8×10^{-4}, 6.4×10^{-4}). Analysis of the NS1 region produced a slightly lower mean substitution rate of 1.9×10^{-4} subs/site/yr (95% HPD 1.1×10^{-4}, 2.8×10^{-4}). These rates are elevated relative to typical DNA viruses in shrimp, yet consistent with earlier region-specific estimates and suggest ongoing evolutionary adaptation in IHHNV (Robles-Sikisaka et al. (2010)).

Support for applying molecular clock models to the capsid region was corroborated by root-to-tip regression analysis in TempEst. For the capsid alignment, the regression produced a slope of 4.2×10^{-4} substitutions per site per year for the capsid region, with an R^2 of 0.27 and correlation coefficient of 0.52 – indicative of a moderate temporal signal. In contrast, the NS1 alignment yielded an R^2 of 0.13 suggesting a low temporal signal for this region under root-to-tip regression. Nevertheless, the BEAST-derived estimated mutation rate for the NS1 region relative to the capsid region is consistent with their respective lengths and the number of identified SNPs.

Estimates of the time to the most recent common ancestor (TMRCA) placed the origin of the included isolates to between 1976 and 1986 (95% HPD), with a mean estimate of approximately 39 years prior to the most recent isolate (2022). These dates align closely with the historical emergence of IHHNV in shrimp aquaculture systems and provide a temporal framework for interpreting subsequent patterns of diversification and spread (Tang et al., 2003).

3.4. Population demography

Historical changes in the global IHHNV effective population size were inferred using a Bayesian Skyline analysis of the capsid and NS1 alignments, with results revealing a broadly consistent demographic trajectory for both datasets (Fig. 2 and Supplementary Fig. 1). From the mid-1980s through the mid-1990s, the effective population size remained relatively stable, followed by a phase of exponential growth between approximately 1995 and 2005.

Population size then plateaued around 2010, suggesting a period of demographic stability.

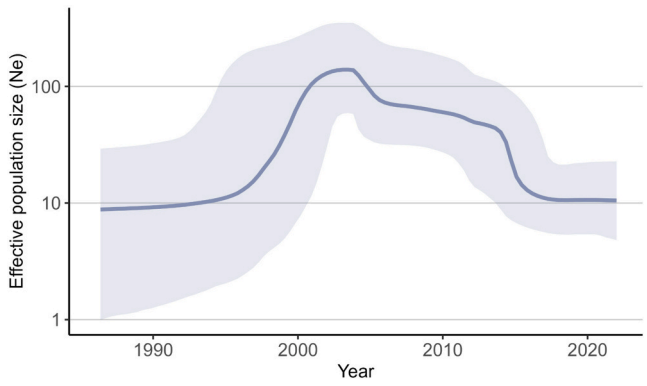

Fig. 2. Bayesian Skyline Plot of IHHNV (Capsid Region). Population dynamics of IHHNV over time, inferred from Bayesian Skyline analysis of the capsid region of 126 sequences, highlighting fluctuations in effective viral population size. The central blue line is the mean effective population size through time, and the shaded region is the 95% highest posterior density interval. (For interpretation of the references to colour in this figure legend, the reader is referred to the web version of this article.)

3.5. Phylogenetic structure and geographic clustering

The maximum clade credibility (MCC) tree inferred from the capsid alignment showed strong geographic structuring, with sequences clustering into distinct, well-supported regional clades (Fig. 3 and 4). These patterns were consistent with results from the NS1 alignment (Supplementary Fig. 2), which displayed a similar topology and reinforced the robustness of the observed phylogenetic structure (Fig. 3 and Supplementary Fig. 2).

All Australian isolates formed a monophyletic clade, with the 19 newly sequenced genomes (2020–2022) clustering with earlier Australian isolates (2008–2019). These sequences shared identical SNP profiles and were genetically distinct from all non-Australian isolates. The Australian isolates showed closest genetic affinity to strains from Taiwan, China, and the Philippines.

A distinct clade comprising isolates from Peru and Ecuador was also identified, with very high sequence similarity and strong support. Two North American isolates – one from Florida (2019) and one from Texas (2019) – were embedded within this clade, indicating a recently shared ancestry. Mexican sequences primarily formed a separate monophyletic group, though a subset clustered with South American and Asian

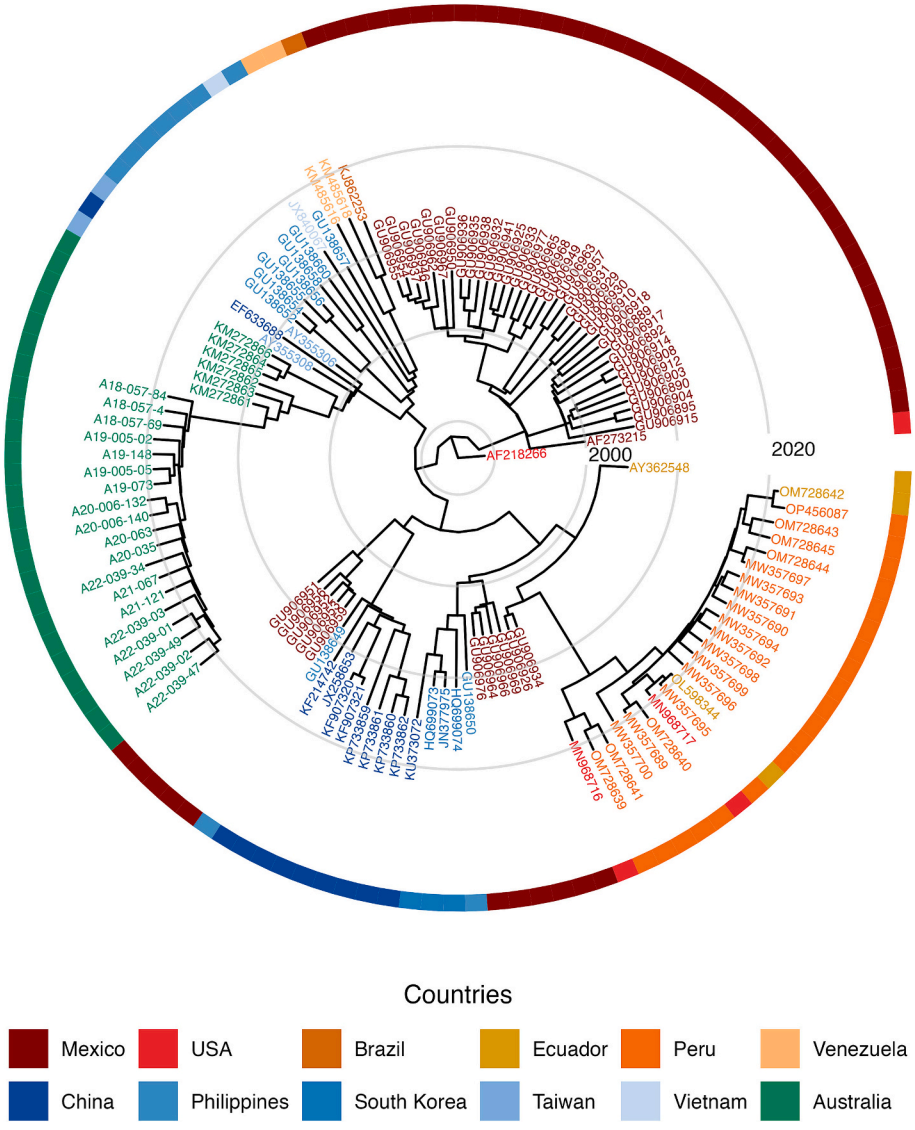

Fig. 3. Maximum Clade Credibility (MCC) time-scaled tree of 126 Global IHHNV Capsid Sequences. Branch lengths are proportional to calendar time. Nodes with low posterior support (<0.80) were collapsed to highlight strongly supported evolutionary patterns among the IHHNV sequences.

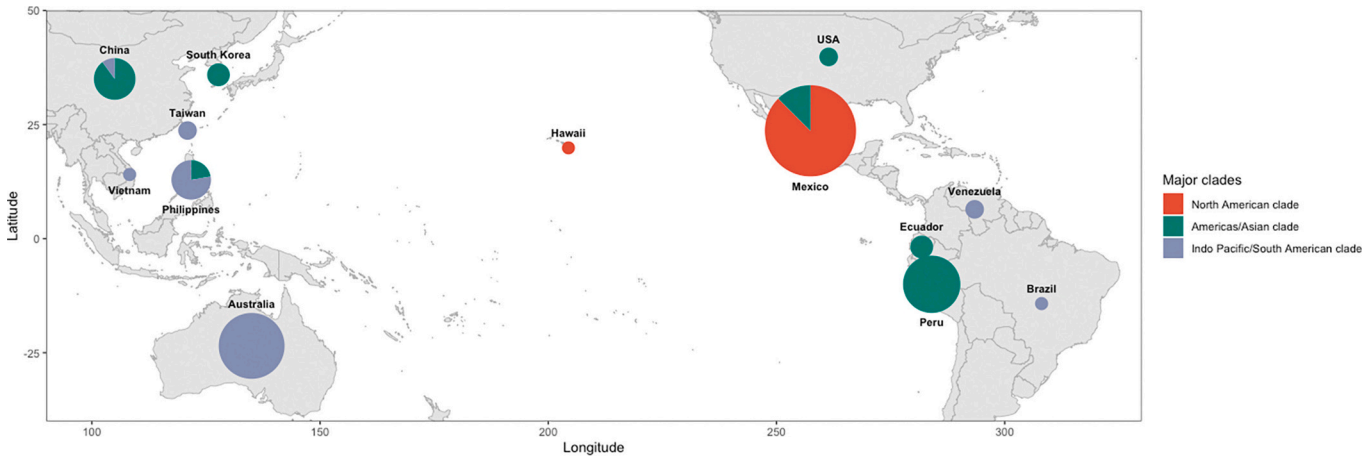

Fig. 4. Global Spatial Distribution of Major IHHNV Clades Represented in this Study. Spatial phylogeography map showing the geographic distribution of IHHNV sequences included in the analysis. Pie charts represent the relative proportion of sequences belonging to each of the three major phylogenetic clades at each sampling location. Radius of pie chartis proportional to the total number of sequences obtained from that region. Clade colours correspond to major clades as described in the legend.

isolates.

Isolates from China and South Korea formed a well-supported clade containing sequences from multiple Chinese provinces (e.g., Shanghai, Ningbo, Wenzhou, Shenyang). The internal structure of this clade showed moderate diversification, with short branch lengths indicating recent common ancestry within subregions.

Posterior support values were high (≥0.80) for major clades, including those representing Australia, Peru–Ecuador, and Mexico. Within-region subclades displayed variable support, reflecting minor genetic divergence.

Branch length variation was consistent with levels of divergence: long branches separated Mexican and Chinese clades from other regions, while short branches within the Peruvian, Australian, and US sequences indicated recent transmission or restricted diversification. Overall, the phylogeny supports strong geographic structure in IHHNV evolution, consistent with pairwise identity data and regional SNP patterns.

4. Discussion and conclusion

Our Bayesian phylogenetic analysis of 126 IHHNV sequences estimated a mean substitution rate of 4.5×10^{-4} (95% HPD $2.8\ 10^{-4}$, 6.4×10^{-4}) substitutions/site/year for the capsid region and 1.9×10^{-4} (95% HPD 1.1×10^{-4}, 2.8×10^{-4}) substitutions/site/year for the NS1 region. Our mutation rate estimate for the capsid region lies within the range of RNA virus mutation rates (10^{-3}–10^{-5}) (Jenkins et al., 2002; Scholtissek, 1995), and although it is higher than the mean rate reported in Kim et al. (2012) (1.25×10^{-4} 95% HPD: 7.153×10^{-9}, 2.629×10^{-4}), it remains within the broader range observed by Robles-Sikisaka et al. (2010) (1.39×10^{-4}, 4.89×10^{-4}) across their explored model configurations. High rates observed in RNA viruses reflect the combination of error-prone RNA dependent polymerases and frequent replication cycles, both of which promote rapid accumulation of substitutions (Jenkins et al., 2002; Scholtissek, 1995). Nevertheless, the higher rate observed in our study may reflect our broader dataset (126 capsid sequences) spanning a longer timeframe (1986–2022) and multiple geographic regions, compared with the smaller (18 capsid sequences collected between 1986 and 2007) dataset used by Robles-Sikisaka et al. (2010). Overall, these findings support the view that IHHNV evolves at RNA virus-like rates, in agreement with growing evidence that small ssDNA viruses can undergo rapid evolutionary change (Duffy et al., 2008; Karunasagar and Ababouch, 2012). Consistent with this, several parvoviruses show similarly elevated rates, for example human parvovirus B19 (2×10^{-4}) (Parsyan et al., 2007), canine parvovirus (CPV) (1.7×10^{-4}) (Shackelton et al., 2005) and the ssDNA porcine circovirus 2 (PCV2) (1.2×10^{-3}) (Firth et al., 2009).

Robles-Sikisaka et al. (2010) estimated the TMRCA to be in the early 1970s. In contrast, our analysis yielded a mean TMRCA of 1983 (95% HPD: 1975–1986). The slightly later timing in our analysis, which was consistently estimated using both the capsid and NS1 regions, is consistent with the higher substitution rate inferred from our dataset.

Phylogenetic reconstruction revealed strong geographic structuring of IHHNV (Fig. 3 and Supplementary Fig. 2). Recent Australian isolates (2018–2022) clustered with earlier local isolates (2008), suggesting long-term persistence and adaptation within regional aquaculture systems. Regional clades also reflect international trade and brood stock movement: Australian isolates shared close similarity with isolates from Taiwan, China and The Philippines while Peruvian, Ecuadorian and US isolates formed a distinct Americas clade. Mexican isolates largely clustered together, although some shared ancestry with Asian and South American strains, implying multiple introduction events or gene flow. Asian isolates displayed higher diversification, likely driven by intense farming and environmental pressures, whereas shorter branches connecting Peruvian isolates indicate recent local transmission events (Fig. 3). Although this study provides valuable information on the global distribution of IHHNV sequences, most samples originate from Mexico, Australia and Peru (Table 1). This uneven sampling introduces a geographic bias, which may influence the inferred phylogenetic relationships and demographic patterns. Regions with few or no samples may appear less diverse or underrepresented and the reconstructed population dynamics could disproportionately reflect trends in the heavily sampled countries. Consequently, interpretations of global evolutionary and demographic patterns of IHHNV should be made cautiously, as the available data may not fully capture diversity in under-sampled regions.

The analysis of 126 capsid sequences identified region-specific SNPs reflecting phylogenetic patterns (Table 2). Key SNPs included positions 125 and 153, primarily observed in Peruvian, Ecuadorian and U.S. isolates, though present in only two Mexican isolates, suggesting limited introduction or shared ancestry. Positions 714 and 965 were exclusive to Australian isolates, while additional SNPs were uniquely observed in Mexican, Chinese and South Korean isolates. SNPs at positions 907 and 908 consistently occurred together, suggesting a linked change. Several of these SNPs are non-synonymous, potentially affecting viral pathogenicity or adaptation. SNPs in the NS1 genome were fewer but showed similar geographic patterns, with most occurring in isolates from the Americas and SNP 1509 largely confined to Australia, reinforcing the regional structuring observed in the capsid gene. Overall, these region-specific SNPs serve as population-specific markers and underscore

localised viral evolution.

BSP analysis revealed the historical population dynamics of IHHNV (Fig. 2), aligning closely with known epizootic events. A relatively low effective population size from 1986 to 1995 reflects early stages of IHHNV emergence, limited viral spread and sparse detection. From the mid–1990s to the mid–2000s, the virus experienced an approximately 10-fold increase in effective population size corresponding with the intensification of shrimp farming, global brood stock movement, and improved surveillance and diagnostic techniques, which may have amplified apparent viral prevalence (Lightner, 1996; Lightner, 1999). From the mid–2000s to 2022, the effective population size decreased by roughly 10-fold, likely reflecting the widespread adoption of SPF (Specific Pathogen-Free) brood stock, improved biosecurity and development of IHHNV-resistant shrimp strains, alongside consistent global sampling (Barman et al., 2012; Jaroenram et al., 2015). It is important to note that periods of heightened sampling and more sensitive diagnostic tools may inflate apparent population size, while decreased detection could result from improved disease management and resistant hosts. While sampling bias may influence trends, these results provide insights into the virus's demographic history and highlight the interplay between human-mediated factors and viral evolution (Fig. 2).

It is noteworthy that analyses of both the NS1 and capsid genomes produced consistent phylogenetic topologies, population size patterns and supported similar estimates of a relatively recent common ancestor. This agreement across genomic regions strengthens the robustness of our findings. The observed high substitution rates, ongoing diversification, and region-specific SNP patterns emphasise the need for continued surveillance and sampling to monitor IHHNV evolution. Regional SNP markers could inform lineage tracing, biosecurity measures and the detection of emerging, potentially more virulent strains. In this context, sensitive and field-deployable diagnostic tools, including ISDL, D-LAMP and real-time triplex LAMP assays (Arunrut et al., 2019; Arunrut et al., 2024; Jitrakorn et al., 2016), will be important to support routine screening and early detection of circulating lineages. International trade, ecological factors, and host adaptation remain key drivers of viral spread and diversification, highlighting the importance of global monitoring in shrimp aquaculture systems.

CRediT authorship contribution statement

Emmanuel Ofori-Amponsah: Writing – review & editing, Writing – original draft, Visualization, Validation, Software, Resources, Methodology, Investigation, Formal analysis, Data curation, Conceptualization. **Maria Andrade Martinez:** Resources, Investigation, Data curation. **Michael T. Meehan:** Writing – review & editing, Supervision, Resources, Project administration, Methodology, Funding acquisition, Conceptualization. **Kelly Condon:** Writing – review & editing, Supervision, Resources, Project administration, Investigation, Data curation, Conceptualization.

Declaration of competing interest

The authors state that they have no financial or personal relationships that could have influenced the work presented in this paper.

Acknowledgement

M.T.M. and E.O.A. are supported by an Australian Research Council Discovery Early Career Researcher Award, DE210101344.

This research is funded by the Cooperative Research Centre for Developing Northern Australia (CRCNA), A.3.2021044, which is supported by the Cooperative Research Centres Program, an Australian Government initiative. The CRCNA also acknowledges the support of its investment partners: the Western Australian, Northern Territory and Queensland Governments. The Australian Prawn Farmers Association and the Fisheries Research and Development Corporation is gratefully acknowledged for their investment support. Australian Prawn Farms, Seafarm and Pacific Reef Tigers are acknowledged for their support in provision of experimental animals.

Appendix A. Supplementary data

Supplementary data to this article can be found online at https://doi.org/10.1016/j.aquaculture.2026.743684.

Data availability

I have shared the link to my data and will make it publicly accessible when manuscript is published.

References

Alday-Sanz, V., Brock, J., Flegel, T.W., McIntosh, R., Bondad-Reantaso, M.G., Salazar, M., Subasinghe, R., 2020. Facts, truths and myths about SPF shrimp in aquaculture. Rev. Aquac. 12 (1), 76–84.

Aranguren Caro, L.F., Gomez-Sanchez, M.M., Piedrahita, Y., Mai, H.N., Cruz-Flores, R., Alenton, R.R.R., Dhar, A.K., 2022. Current status of infection with infectious hypodermal and hematopoietic necrosis virus (IHHNV) in the Peruvian and Ecuadorian shrimp industry. PLoS One 17 (8), e0272456. https://doi.org/10.1371/journal.pone.0272456.

Arbon, P., Condon, K., Martinez, M.A., Jerry, D., 2022. Molecular detection of six viral pathogens from Australian wild sourced giant black tiger shrimp (*Penaeus monodon*) broodstock. Aquaculture 548, 737651. https://doi.org/10.1016/j.aquaculture.2021.737651.

Arunrut, N., Jitrakorn, S., Saksmerprome, V., Kiatpathomchai, W., 2019. Double-loop-mediated isothermal amplification (D-LAMP) using colourimetric gold nanoparticle probe for rapid detection of infectious *Penaeus stylirostris* densovirus (PstDNV) with reduced false-positive results from endogenous viral elements. Aquaculture 510, 131–137. https://doi.org/10.1016/j.aquaculture.2019.05.049.

Arunrut, N., Jitrakorn, S., Tondee, B., Saksmerprome, V., Kiatpathomchai, W., 2024. Real-time triplex loop-mediated isothermal amplification (LAMP) using a turbidimeter for detection of shrimp infectious hypodermal and hematopoietic necrosis virus (IHHNV). J. Aquat. Anim. Health 36 (3), 205–219. https://doi.org/10.1002/aah.10218.

Bajaña, L., Betancourt, I., Bayot, B., 2022. Complete coding genome sequence of infectious hypodermal and hematopoietic necrosis virus isolated from *Penaeus (Litopenaeus) vannamei* shrimp in Ecuador. Microbiol. Resource Announce. 11 (4), e01143-01121.

Barman, D., Kumar, V., Roy, S., Mandal, S.C., 2012. Specific pathogen free shrimps: their scope in aquaculture. World Aquac. 43 (1), 67.

Belak, J., Dhar, A.K., Primavera, J.H., de la Pena, L.D., Pettit, P., Alcivar-Warren, A., 1998. Prevalence of viral diseases (IHHNV and WSSV) in *Penaeus monodon* from the philippines and its association with mangrove status and shrimp culture systems. In: Symposium on Aquaculture and Conservation of Marine Shrimp Biodiversity. Tufts University School of Veterinary Medicine, Massachusetts, USA.

Bell, T.A., Lightner, D., 1984. IHHN virus: infectivity and pathogenicity studies in *Penaeus stylirostris* and *Penaeus vannamei*. Aquaculture 38 (3), 185–194. https://doi.org/10.1016/0044-8486(84)90142-X.

Bouckaert, R., Vaughan, T.G., Barido-Sottani, J., Duchêne, S., Fourment, M., Gavryushkina, A., et al., 2019. BEAST 2.5: An advanced software platform for Bayesian evolutionary analysis. PLoS Comput. Biol. 15 (4), e1006650.

Canada, G.o., 2019. Fact Sheet—Infectious Hypodermal and Haematopoitic Necrosis, p. 2019. Retrieved from. https://inspection.canada.ca/animal-health/aquatic-animals/diseases/immediately-notifiable/infectious-hypodermal-and-haematopoitic-necrosis/eng/1562271424092/1562271424389#shr-pg0.

Castille, F., Samocha, T., Lawrence, A., He, H., Frelier, P., Jaenike, F., 1993. Variability in growth and survival of early postlarval shrimp (*Penaeus vannamei* Boone 1931). Aquaculture 113 (1–2), 65–81. https://doi.org/10.1016/0044-8486(93)90341-U.

CEFAS, 2019. International Database on Aquatic Animal DISEASE: Infectious Hypodermal and Haematopoietic Necrosis. CEFAS, United Kingdom. https://www.cefas.co.uk/international-database-on-aquatic-animal-diseases/abstract/?id=1938.

Chayaburakul, K., Nash, G., Pratanpipat, P., Sriurairatana, S., Withyachumnarnkul, B., 2004. Multiple pathogens found in growth-retarded black tiger shrimp *Penaeus monodon* cultivated in Thailand. Dis. Aquat. Org. 60, 89–96. https://doi.org/10.3354/dao060089.

Cowley, J.A., Rao, M., Coman, G.J., 2018. Real-time PCR tests to specifically detect IHHNV lineages and an IHHNV EVE integrated in the genome of *Penaeus monodon*. Dis. Aquat. Org. 129 (2), 145–158. https://doi.org/10.3354/dao03243.

Dhar, A.K., Cruz-Flores, R., Caro, L.F.A., Siewiora, H.M., Jory, D., 2019. Diversity of single-stranded DNA containing viruses in shrimp. VirusDisease 30, 43–57. https://doi.org/10.1007/s13337-019-00528-3.

Dhar, A., Cruz-Flores, R., Warg, J., Killian, M., Orry, A., Ramos, J., Garfias, M., Lyons, G., 2022. Genetic relatedness of infectious hypodermal and hematopoietic necrosis virus isolates, United States, 2019. Emerg. Infect. Dis. J. 28 (2), 373. https://doi.org/10.3201/eid2802.211874.

dos Santos Braz, R.D.F., Reis, L.G., Martins, P.C.C., de Sales, M.P., Meissner, R.V., 2009. Prevalence of infectious hypodermal and hematopoietic necrosis virus (IHHNV) in *Penaeus vannamei* cultured in northeastern Brazil. Aquaculture 288 (1–2), 143–146.
Duffy, S., Shackelton, L.A., Holmes, E.C., 2008. Rates of evolutionary change in viruses: patterns and determinants. Nat. Rev. Genet. 9 (4), 267–276.
Fajardo, C., Rodulfo, H., Rodriguez, M., Puig, J., De Donato, M., 2015. Molecular characterization of strains of decapod penstyldensovirus 1 (PstDV1) isolated in farmed *Litopenaeus vannamei* from Venezuela. Aquaculture 436, 34–39. https://doi.org/10.1016/j.aquaculture.2014.10.043.
Firth, C., Charleston, M.A., Duffy, S., Shapiro, B., Holmes, E.C., 2009. Insights into the evolutionary history of an emerging livestock pathogen: porcine circovirus 2. J. Virol. 83 (24), 12813–12821. https://doi.org/10.1128/jvi.01719-09.
Fulks, W., 1992. Diseases of Cultured Penaeid Shrimp.The Oceanic. Institute, Honolulu, Hawaii.
Hasegawa, M., Kishino, H., Yano, T.-A., 1985. Dating of the human-ape splitting by a molecular clock of mitochondrial DNA. J. Mol. Evol. 22 (2), 160–174.
Holmes, E.C., 2011. The evolution of endogenous viral elements. Cell Host Microbe 10 (4), 368–377. https://doi.org/10.1016/j.chom.2011.09.002.
Hsia, H.-L., Chen, L.-L., Peng, S.-E., Yu, H.-T., Lo, C.-F., Kou, G.-H., 2003. Comparison of genomic sequence of infectious hypodermal and hematopoietic necrosis virus (IHHNV) between Taiwan and other geographical isolates. Fish Pathol 38 (4), 177–179. https://doi.org/10.3147/jsfp.38.177.
Jaroenram, W., Owens, L., 2014. Separation of endogenous viral elements from infectious *Penaeus stylirostris* densovirus using recombinase polymerase amplification. Mol. Cell. Probes 28 (5–6), 284–287. https://doi.org/10.1016/j.mcp.2014.08.002.
Jaroenram, W., Chaivisuthangkura, P., Owens, L., 2015. One base pair deletion and high rate of evolution: keys to viral accommodation of Australian *Penaeus stylirostris* densovirus. Aquaculture 443, 40–48. https://doi.org/10.1016/j.aquaculture.2015.03.003.
Jenkins, G.M., Rambaut, A., Pybus, O.G., Holmes, E.C., 2002. Rates of molecular evolution in RNA viruses: a quantitative phylogenetic analysis. J. Mol. Evol. 54, 156–165. https://doi.org/10.1007/s00239-001-0064-3.
Jitrakorn, S., Arunrut, N., Sanguanrut, P., Flegel, T.W., Kiatpathomchai, W., Saksmerprome, V., 2016. In situ DIG-labeling, loop-mediated DNA amplification (ISDL) for highly sensitive detection of infectious hypodermal and hematopoietic necrosis virus (IHHNV). Aquaculture 456, 36–43. https://doi.org/10.1016/j.aquaculture.2016.01.023.
Karunasagar, I., Ababouch, L., 2012. Shrimp viral diseases, import risk assessment and international trade. Indian J. Virol. 23, 141–148. https://doi.org/10.1007/s13337-012-0081-4.
Kim, J.H., Choresca Jr., C.H., Shin, S.P., Han, J.E., Jun, J.W., Han, S.Y., Park, S.C., 2011. Detection of infectious hypodermal and hematopoietic necrosis virus (IHHNV) in *Litopenaeus vannamei* shrimp cultured in South Korea. Aquaculture 313 (1–4), 161–164. https://doi.org/10.1016/j.aquaculture.2011.01.019.
Kim, J., Kim, H., Nguyen, V., Park, B., Choresca, C., Shin, S., Han, J., Jun, J., Park, S., 2012. Genomic sequence of infectious hypodermal and hematopoietic necrosis virus (IHHNV) KLV-2010-01 originating from the first Korean outbreak in cultured *Litopenaeus vannamei*. Arch. Virol. 157, 369–373. https://doi.org/10.1007/s00705-011-1155-0.
Krabsetsve, K., Cullen, B.R., Owens, L., 2004. Rediscovery of the Australian strain of infectious hypodermal and haematopoietic necrosis virus. Dis. Aquat. Org. 61 (1–2), 153–158. https://doi.org/10.3354/dao061153.
Lightner, D., 1992a. A collection of case histories documenting the introduction and spread of the virus disease IHHN in penaeid shrimp culture facilities in northwestern Mexico. ICES Mar. Sci. Symp. 194, 97–105.
Lightner, D., 1992b. New Developments in Penaeid Virology: Application of Biotechnology in Research and Disease Diagnosis for Shrimp Viruses of Concern in the Americas. In: Fulks, W., Main, K. (Eds.). Publ. by The Oceanic Institute, Makapuu Point, Honolulu, pp. 233–263 (Disease of Cultured Penaeid Shrimp in Asia and the United States).
Lightner, D., 1996. Epizootiology, production impacts and role of international trade in their distribution in the Americas. Rev. Sci. Techn. Off. Int. Epiz. 15 (2), 579–601.
Lightner, D.V., 1999. The penaeid shrimp viruses TSV, IHHNV, WSSV, and YHV: current status in the Americas, available diagnostic methods, and management strategies. J. Appl. Aquac. 9 (2), 27–52. https://doi.org/10.1300/J028v09n02_03.
Lightner, D., Redman, R., Bell, T., Brock, J., 1983. Detection of IHHN virus in *Penaeus stylirostris* and *P. Vannamei* imported into Hawaii. J. World Maricult. Soc. 14 (1–4), 212–225. https://doi.org/10.1111/j.1749-7345.1983.tb00077.x.
Mari, J., Bonami, J.-R., Lightner, D., 1993. Partial cloning of the genome of infectious hypodermal and haematopoietic necrosis virus, an unusual parvovirus pathogenic for penaeid shrimps; diagnosis of the disease using a specific probe. J. Gen. Virol. 74 (12), 2637–2643. https://doi.org/10.1099/0022-1317-74-12-2637.
Owens, L., 1992. Infectious hypodermal and haematopoetic necrosis virus (IHHNV) in an interspecies hybrid penaeid prawn from tropical Australia. Dis. Aquat. Org. 14, 219–228. https://doi.org/10.3354/dao014219.
Parsyan, A., Szmaragd, C., Allain, J.-P., Candotti, D., 2007. Identification and genetic diversity of two human parvovirus B19 genotype 3 subtypes. J. Gen. Virol. 88 (2), 428–431. https://doi.org/10.1099/vir.0.82496-0.
Praveen Rai, P.R., Balakrishnan Pradeep, B.P., Iddya Karunasagar, I.K., Indrani Karunasagar, I.K., (2009). Detection of Viruses in *Penaeus monodon* from India Showing Signs of Slow Growth Syndrome. Aquaculture, 289, 231-235.
Primavera, J.H., Quinitio, E.T., 2000. Runt-deformity syndrome in cultured giant tiger prawn *Penaeus monodon*. J. Crustac. Biol. 20 (4), 796–802. https://doi.org/10.1163/20021975-99990101.
Rai, P., Safeena, M.P., Krabsetsve, K., La Fauce, K., Owens, L., Karunasagar, I., 2012. Genomics, molecular epidemiology and diagnostics of infectious hypodermal and hematopoietic necrosis virus. Indian J. Virol. 23, 203–214. https://doi.org/10.1007/s13337-012-0083-2.
Rambaut, A., Lam, T.T., Max Carvalho, L., Pybus, O.G., 2016. Exploring the temporal structure of heterochronous sequences using TempEst (formerly path-O-gen). Virus Evol. 2 (1), vew007. https://doi.org/10.1093/ve/vew007.
Robles-Sikisaka, R., Bohonak, A.J., McClenaghan Jr., L.R., Dhar, A.K., 2010. Genetic signature of rapid IHHNV (infectious hypodermal and hematopoietic necrosis virus) expansion in wild *Penaeus shrimp* populations. PLoS One 5 (7), e11799. https://doi.org/10.1371/journal.pone.0011799.
Saksmerprome, V., Puiprom, O., Noonin, C., Flegel, T.W., 2010. Detection of infectious hypodermal and haematopoietic necrosis virus (IHHNV) in farmed Australian *Penaeus monodon* by PCR analysis and DNA sequencing. Aquaculture 298 (3–4), 190–193. https://doi.org/10.1016/j.aquaculture.2009.11.012.
Salcedo-Mejía, L.A., Durán-Ramirez, Y., Velazco-Peña, R.Z., Pinto, J.A., Rebaza-Caballero, A., 2021. Near-complete genome sequences of 12 Peruvian strains of infectious hypodermal and hematopoietic necrosis virus infecting the shrimp *Penaeus vannamei*. Microbiol. Resource Announce. 10 (20), 00169-00121. https://doi.org/10.1128/mra.
Scholtissek, C., 1995. Molecular evolution of influenza viruses. Virus Genes 11, 209–215.
Shackelton, L.A., Parrish, C.R., Truyen, U., Holmes, E.C., 2005. High rate of viral evolution associated with the emergence of carnivore parvovirus. Proc. Natl. Acad. Sci. 102 (2), 379–384. https://doi.org/10.1073/pnas.0406765102.
Shike, H., Dhar, A.K., Burns, J.C., Shimizu, C., Jousset, F.X., Klimpel, K.R., Bergoin, M., 2000. Infectious hypodermal and hematopoietic necrosis virus of shrimp is related to mosquito brevidensoviruses. Virology 277 (1), 167–177. https://doi.org/10.1006/viro.2000.0589.
Silva, D.C., Nunes, A.R., Teixeira, D.I., Lima, J.P.M., Lanza, D.C., 2014. Infectious hypodermal and hematopoietic necrosis virus from Brazil: sequencing, comparative analysis and PCR detection. Virus Res 189, 136–146. doi.org/10.1016/j.virusres.2014.05.008.
Sunarto, A., Koesharyani, I., Supriyadi, H., Gardenia, L., Sugianti, B., Rukmono, D., 2004. Current status of transboundary fish diseases in Indonesia: occurrence, surveillance, research and training. Transboundary fish diseases in Southeast Asia: occurence, surveillance, research and training. In: Proceedings of the Meeting on Current Status of Transboundary Fish Diseases in Southeast Asia: Occurence, Surveillance, Research and Training, Manila, Philippines, 23-24 June 2004.
Tang, K.F., Lightner, D.V., 2006. Infectious hypodermal and hematopoietic necrosis virus (IHHNV)-related sequences in the genome of the black tiger prawn *Penaeus monodon* from Africa and Australia. Virus Res 118 (1–2), 185–191. https://doi.org/10.1016/j.virusres.2006.01.003.
Tang, K.F., Poulos, B.T., Wang, J., Redman, R.M., Shih, H.-H., Lightner, D.V., 2003. Geographic variations among infectious hypodermal and hematopoietic necrosis virus (IHHNV) isolates and characteristics of their infection. Dis. Aquat. Org. 53 (2), 91–99. https://doi.org/10.3354/dao053091.
Tang, K.F.J., Lavilla-Pitogo, C.R., Lightner, D.V., 2009. Detection of Infectious Hypodermal and Hematopoietic Necrosis Virus (IHHNV) in Introduced, Farmed Penaeus Vannamei and Native Penaeids from the Philippines. University of Arizona.
Wei, Y.-W., Fan, D.-D., Chen, J., 2015. Development of an overlapping PCR method to clone the full genome of infectious hypodermal and hematopoietic necrosis virus (IHHNV). J. Virol. Methods 224, 16–19.
Wyban, J., 2007. Domestication and Globalization of Specific Pathogen Free (SPF) *Penaeus vannamei*.In I Chiu Liao, Nai-Hsien Chao and Eduardo M. Leaño Eds. Progress of Shrimp and Prawn Aquaculture in the World. National Taiwan Ocean University, Keelung, Taiwan, The Fisheries Society of Taiwan, Keelung, Taiwan, Asian Fisheries Society, Manila, Philippines, and World Aquaculture Society, Louisiana, USA. p.111-125.
Xia, X., Yu, Y., Hu, L., Weidmann, M., Pan, Y., Yan, S., Wang, Y., 2015. Rapid detection of infectious hypodermal and hematopoietic necrosis virus (IHHNV) by real-time, isothermal recombinase polymerase amplification assay. Arch. Virol. 160 (4), 987–994. https://doi.org/10.1007/s00705-015-2357-7.
Yu, J.-Y., Yang, N., Hou, Z.-H., Wang, J.-J., Li, T., Chang, L.-R., Fang, Y., Yan, D.-C., 2021. Research progress on hosts and carriers, prevalence, virulence of infectious hypodermal and hematopoietic necrosis virus (IHHNV). J. Invertebr. Pathol. 183, 107556. https://doi.org/10.1016/j.jip.2021.107556.
Zhong, X., Yuan, J., Zhang, X., Li, S., Liu, C., Si, S., Hu, J., Prachumwat, A., Sritunyalucksana, K., Li, F., 2025. Dynamic integration and evolutionary trajectory of endogenous IHHNV elements in crustacean genomes. DNA Res. 32 (4), dsaf018. https://doi.org/10.1093/dnares/dsaf018.
Yang, Bing, Song, XiaoLing, Huang, Jie, Shi, ChengYin, Li, Liu, 2007. Evidence of Existence of Infectious Hypodermal and Hematopoietic Necrosis Virus in Penaeid Shrimp Cultured in China. Vet. Microbiol. 120, 63–70. https://doi.org/10.1016/j.vetmic.2006.10.011.